

Filter properties of nano cylindrical electronic substances

Abhishek Tiwari

**Department of Physics (Applied Sciences)*
 SRIMT, DR APJ Abdul Kalam Technical University
 Lucknow, (UP) 226201
 India

Abstract—CNTs are attractive materials in fundamental science and technology. They have demonstrated unique electrical properties for building electronic devices, such as CNT field-effect transistors (CNTFETs) and CNT diodes. CNTs can be used to form a p–n junction diode by chemical doping and polymer coating. These types of diodes can be used to form a computer chip. CNT diodes can potentially dissipate heat out of the computer chips due to their unique thermal transmission properties (Jorio et al. 2008). There is also a remarkable tendency of nano size substance that they can act as filters. This property is marvelous and is being deployed for nano-sensors. Here is a study of filtration behavior of materials and their comparison.

Index Terms—cnts, high-pass and low pass filters, surface coupled modes.

I. INTRODUCTION

Discoveries of very constant nanometer size sp^2 carbon bonded materials such as graphene [1], fullerenes [2], and carbon nanotubes [3] have encouraged to make inquiries in this field. Most of the physical properties of carbon nanotubes derive from graphene. Applications for nanotubes encompass many fields and disciplines such as medicine, nanotechnology, manufacturing, construction, electronics, and so on. The following application can be noted: high-strength composites [4,5-10], actuators [11], energy storage and energy conversion devices [12], nanopores and sensors [13], hydrogen storage media [14], electronic devices [15], and catalysis [16]. The unique electronic properties of carbon nanotube are due to the quantum confinement of electrons normal to the nanotube axis. In the radial direction, electrons are confined by monolayer thickness of graphene sheet. Around the circumference of the nanotube, periodic boundary condition comes into play. In order to study this coupling the dispersion relation can be obtained by various methods. The hydrodynamical model is one of the various methods to study the behavior of polariton, phonon on the geometrical surface of materials.

II. FILTERING PROPERTIES AND THEIR ANALYSIS

The dielectric function $\epsilon_L(\omega)$, for a polar semiconductor, due to the lattice, is given by,

$$\epsilon_L(\omega) = \left(\frac{\epsilon_\infty \omega^2 - \epsilon_0}{\omega^2 - 1} \right) \quad (1)$$

In terms of the reduced frequency $\omega \left(= \frac{\omega}{\omega_t} \right)$ may be written as:

$$\epsilon_L(\omega) = \left(\frac{\epsilon_\infty \omega^2 - \epsilon_0}{\omega^2 - 1} \right) \quad (2)$$

The plot of ' $\epsilon_L(\omega)$ ' vs. ' ω ' is shown in the fig (1-4).

The curve ' $\epsilon_L(\omega)$ ' has a pole at $\omega=1$, i.e., at $\omega = \omega_t$, which is the transverse optical phonon frequency. For $1 < \omega < 1.1$, the values of $\epsilon_L(\omega)$ are negative and it becomes zero at $\omega=1.1$.

From equ. (2), $\epsilon_L(\omega)=0$ implies that

$$\omega^2 = \frac{\epsilon_0}{\epsilon_\infty} \tag{3}$$

Or $\omega^2 = \frac{\epsilon_0}{\epsilon_\infty} \omega_t^2 = \omega_\ell^2$ (4)

by using the Lyddane-Sachs-Teller equation. Here ‘ ω_ℓ ’ is the longitudinal optical phonon frequency.

Thus, the lattice dielectric function remains negative in the frequency range between ‘ ω_t ’ and ‘ ω_ℓ ’

Also, the value $\epsilon_L(\omega)=-1$ corresponds to $\omega=1.09$ from the graph. This is actually the surface mode frequency given by eq. $\omega = \sqrt{\frac{1 + \epsilon_0}{1 + \epsilon_\infty}}$ for InAs. At this frequency, the refractive index ‘n’

of the medium tends to infinity. The dependence of ‘n’ on frequency is discussed in the following section.

The frequency dependent lattice-dielectric function $\epsilon_L(\omega)$ given by eq. (2) is plotted for InSb, GaP, GaAs, and SiC.

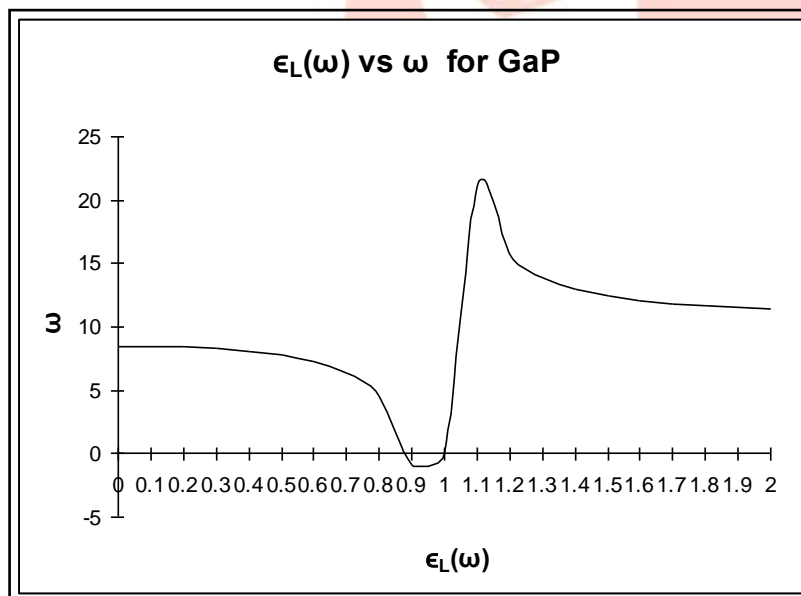


Fig.1

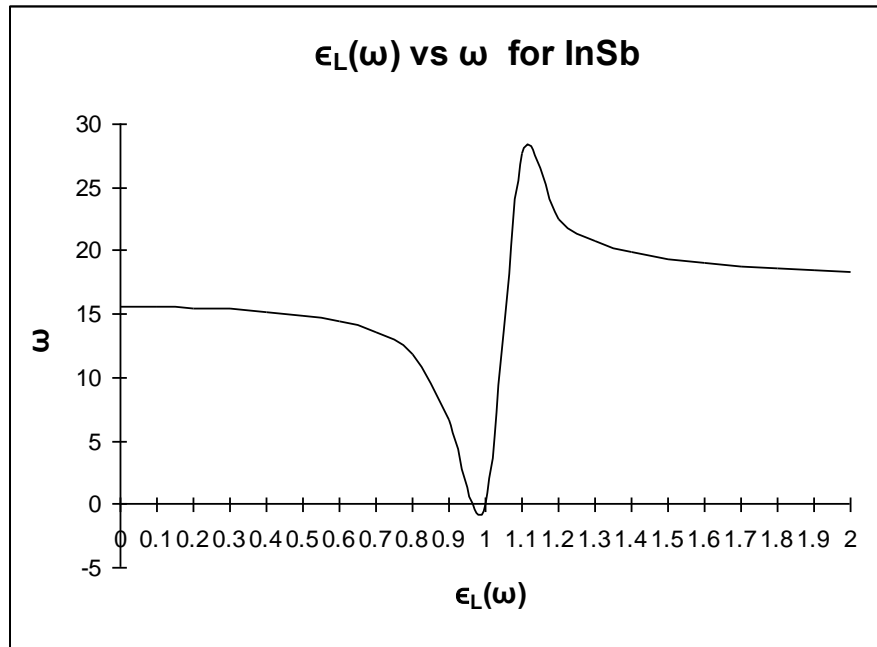


Fig.2

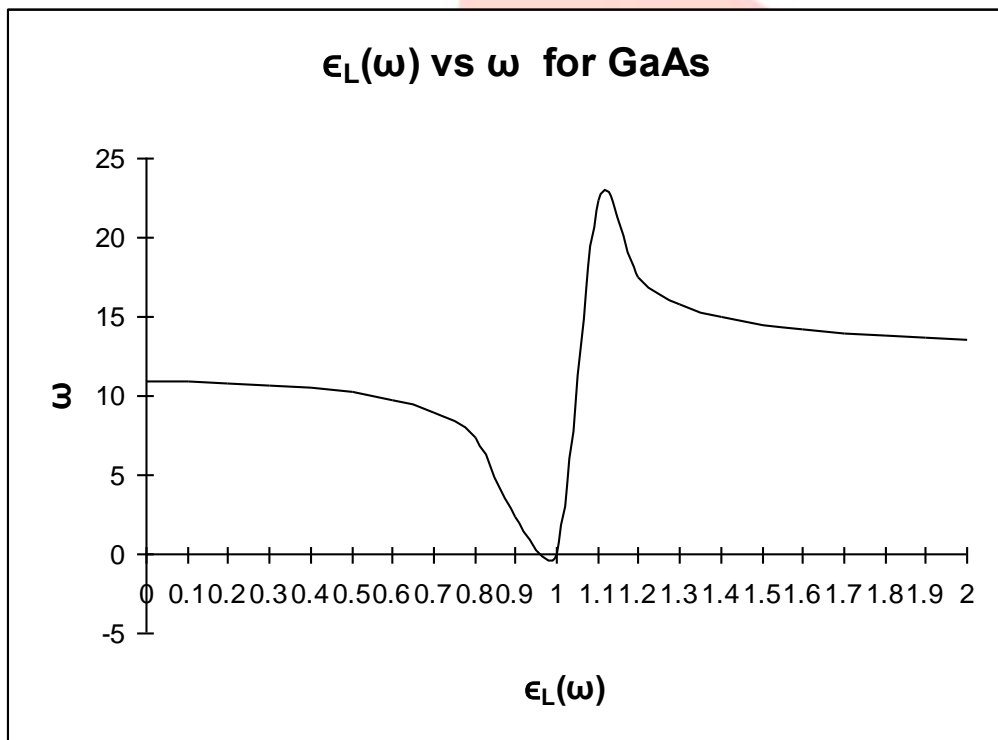


Fig.3

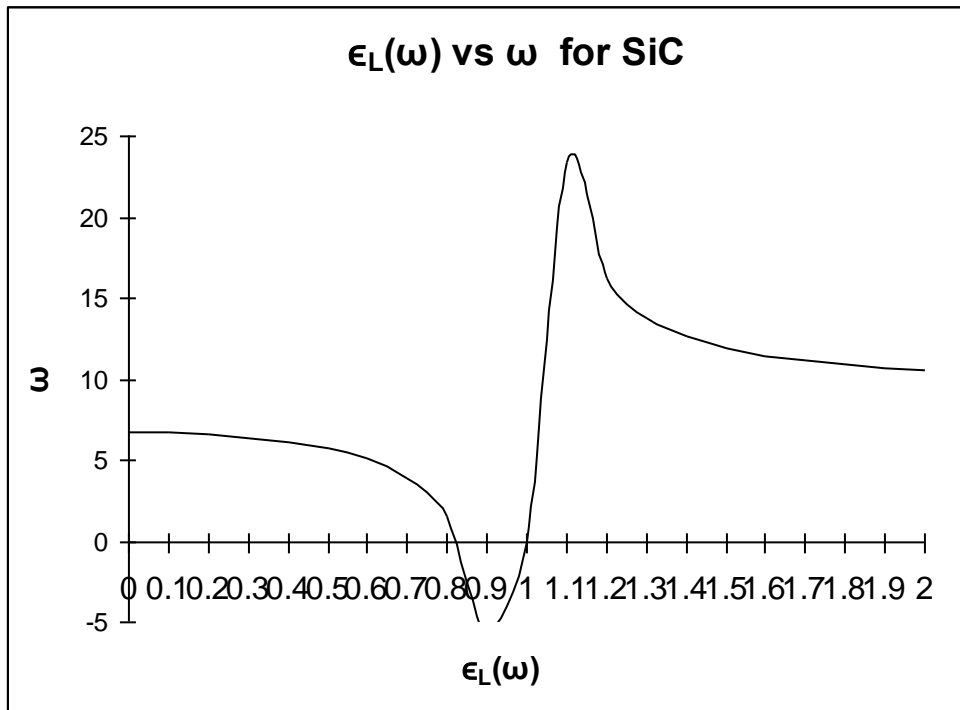


Fig.4

A plot of equation $\epsilon_B \epsilon_\infty \omega^4 - [\epsilon_B \epsilon_0 + (\epsilon_B + \epsilon_\infty) k_1^2] \omega^2 + (\epsilon_B + \epsilon_0) k_1^2 = 0$ taking $\epsilon_B = 1$ fig. (1-4) again gives two coupled surface modes, the lower being the non-radiative, bound surface modes which tends pure photon mode for low values of wave vector, and to the surface optical phonon frequency for high values of wave vector, and show a mixed surface phonon-photon character for intermediate values of wave vector. The lattice dielectric function $\epsilon_L(\omega)$, given by equation

$$\Omega^6 \left(\frac{\omega_p}{\omega_t} \right)^2 \epsilon_\infty - \left[\epsilon_0 + \left\{ \bar{\epsilon} + (1 + \epsilon_\infty) k^2 \right\} \left(\frac{\omega_p}{\omega_t} \right)^2 \right] \Omega^4 + \left[\left\{ (1 + \epsilon_0) + \bar{\epsilon} \left(\frac{\omega_p}{\omega_t} \right)^2 \right\} k^2 + \bar{\epsilon} \right] \Omega^2 - \bar{\epsilon} k^2 = 0 \tag{5}$$

Whose frequency dependence results in surface optical phonon waves at the surface of polar semiconductor, and the corresponding values of $n^2 (\phi_l(r, t) = \sum_l \phi_l(r) Y_l(\theta) e^{i(k \cdot r - \omega t)})$ have also been plotted (figures). From the analysis of fig. 1-4 along with the fig.5 it is clear that the incident E.M. wave will be transmitted for $\omega < 1.0$ and $\omega > 1.1$.

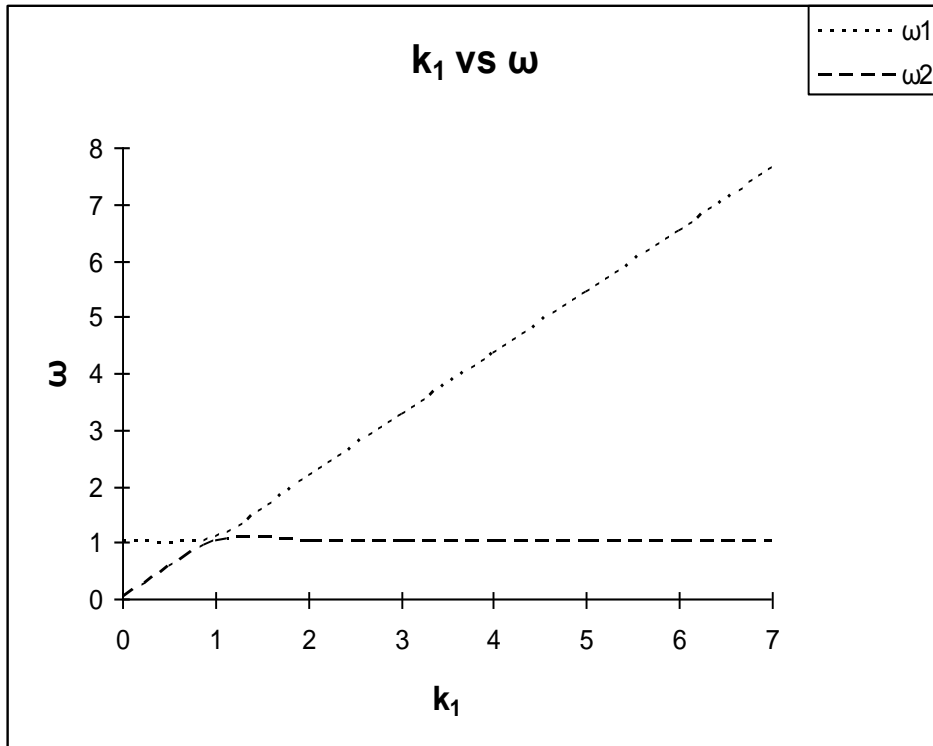


Fig.5

Thus, the surface of a polar semiconductor, in this case, acts a low pass and high pass filter for the incident E.M. wave.

III. RESULTS

Result of fig.1-4 for low pass and high pass filter for nanoscale measurement of cylindrical polar semiconductor.

Result

	InSb	GaP	GaAs	SiC
$\epsilon_{L1}(\omega) / \omega_1$.95/0	.9/0	.95/0	.9/0
$\epsilon_{L2}(\omega) / \omega_2$	1/1	1.0/0	1.0/0	1.0/0
$\epsilon_{L3}(\omega) / \omega_3$.7/13.58235	6.38627/.7	.7/8.9784	.7/3.9137
$\epsilon_{L4}(\omega) / \omega_4$	1.2/27.7	1.2/21.17619	1.2/22.423	1.1/23.409

Table for Dielectrice constant ϵ_L VFS. ω / ω_t

ω	MgO	InP	Carbon
0.2	10.875	12.51667	5.5
0.4	11.11429	12.93333	5.5
0.6	13.68125	13.975	5.5
0.8	22.06687	17.37778	5.5
01	∞	∞	∞
1.2	- 12.7818	3.236364	5.5
1.4	-4.2875	6.683333	5.5
1.6	-1.52308	7.805128	5.5
1.8	-0.18036	8.35	5.5
02	8.666667	5.5
2.2	8.870833	5.5
2.4	9.011765	5.5
2.6	9.113889	5.5
2.8	9.190643	5.5

Further if graph is plotted between dielectric constant and ω / ω_t it comes to be as the following

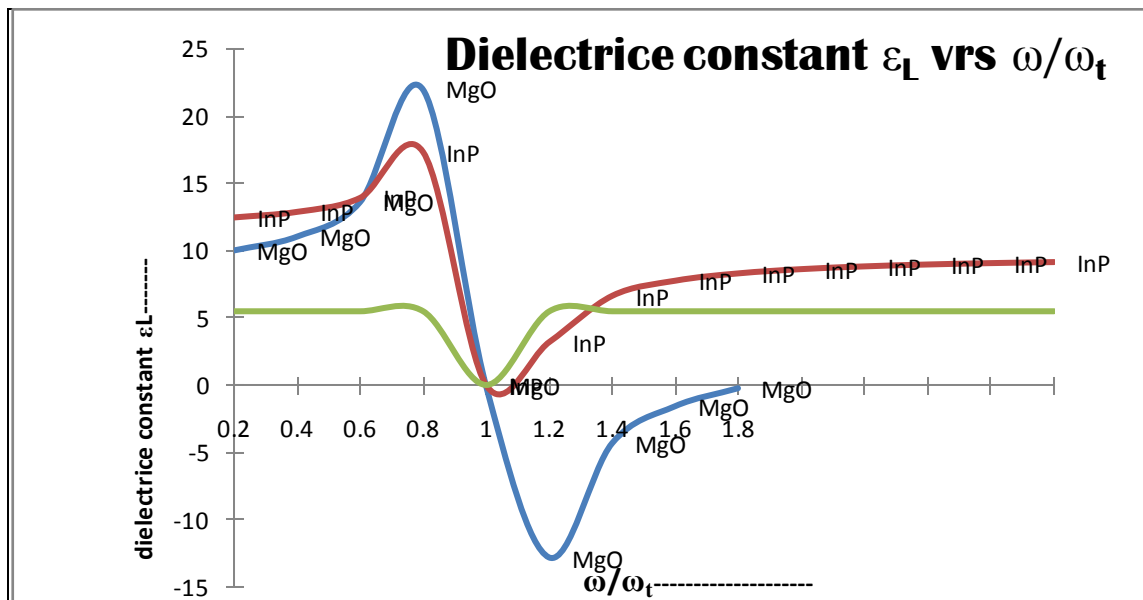


Fig. 6

IV. CONCLUSIONS

Now taking $\epsilon_B = 1$ fig (6) again gives two coupled surface modes, the lower being the non – radiative, bound surface modes which tends pure photon mode for low values of wave vector, and to the surface optical phonon frequency for high values of wave vector, and show a mixed surface phonon–photon character for intermediate values of wave vector. The lattice dielectric function $\epsilon_L(\omega)$, given by [Whose frequency dependent results in surface optical phonon waves at the surface of polar semiconductor], and the corresponding values of n^2 have also been plotted. From the analysis of fig along with the other figure it is clear that the incident EM wave will be transmitted for $\omega < 1.0$ and $\omega > 1.1$. Thus the surface of a polar semiconductor, in this case, acts a low pass and high pass filter for the incident EM wave.

V. ACKNOWLEDGMENT

The authors would like to acknowledge the supports of institute to give assistance and facilities .

REFERENCES

1. Ouyang M, Huang JL, Cheung CL, Lieber CM. Atomically resolved single-walled carbon nanotube intramolecular junctions. *Science*. 2001;9(5501):97–100. [[PubMed](#)]
2. Kim H, Lee J, Kahng SJ, Son YW, Lee SB, Lee CK, Ihm J, Kuk Y. Direct observation of localized defect states in semiconductor nanotube junctions. *Phys Rev Lett*. 2003;9(21):216107. [[PubMed](#)]
3. Chico L, Crespi VH, Benedict LX, Louie SG, Cohen ML. Pure carbon nanoscale devices: nanotube heterojunctions. *Phys Rev Lett*. 1996;9(6):971–974. [[PubMed](#)]
4. Huang X, Mclean RS, Zheng M. High-resolution length sorting and purification of DNA-wrapped carbon nanotubes by size-exclusion chromatography. *Anal Chem*. 2005;9(19):6225–6228. [[PubMed](#)]
5. Hersam MC. Progress towards monodisperse single-walled carbon nanotubes. *Nat Nanotechnol*. 2008;9(7):387–394. [[PubMed](#)]
6. Rinzler AG, Liu J, Dai H, Nikolaev P, Huffman CB, Rodriguez-Macias FJ, Boul PJ, Lu AH, Heymann D, Colbert DT. Large-scale purification of single-wall carbon nanotubes: process, product, and characterization. *Appl Phys A Mater Sci Process*. 1998;9(1):29–37.
7. Gu Z, Peng H, Hauge RH, Smalley RE, Margrave JL. Cutting single-wall carbon nanotubes through fluorination. *Nano Lett*. 2002;9(9):1009–1013.
8. Popov VN. Carbon nanotubes: properties and application. *Materials Science and Engineering: R: Reports*. 2004;9(3):61–102.

9. Baughman RH, Zakhidov AA, de Heer WA. Carbon nanotubes—the route toward applications. *Science*. 2002;9(5582):787–792. [[PubMed](#)]
10. Terrones M. Science and technology of the twenty-first century: synthesis, properties, and applications of carbon nanotubes. *Annu Rev Mater Res*. 2003;9(1):419–501.
11. Dai H, Wong EW, Lu YZ, Fan S, Lieber CM. Synthesis and characterization of carbide nanorods. *Nature*. 1995;9(6534):769–772.
12. Ajayan PM, Zhou OZ. *Carbon nanotubes*. China: Springer; 2001. Applications of carbon nanotubes; pp. 391–425.
13. deHeer WA. Nanotubes and the pursuit of applications. *MRS Bull*. 2004;9(04):281–285.
14. Han W, Fan S, Li Q, Hu Y. Synthesis of gallium nitride nanorods through a carbon nanotube-confined reaction. *Science*. 1997;9(5330):1287–1289.
15. Ye X, Lin Y, Wang C, Wai CM. Supercritical fluid fabrication of metal nanowires and nanorodstemplated by multiwalled carbon nanotubes. *Adv Mater*. 2003;9(4):316–319.
16. Bower C, Rosen R, Jin L, Han J, Zhou O. Deformation of carbon nanotubes in nanotube—polymer composites. *ApplPhys Lett*. 1999;9(22):3317–3319.

